A SIMPLIFIED METHOD FOR PREDICTING THE STABILITY OF AERODYNAMICALLY EXCITED TURBOMACHINERY

Albert F. Storace
General Electric Aircraft Engines
Cincinnati, Ohio, U.S.A.

A method is presented for the quick and accurate prediction of the stability of aerodynamically excited turbomachinery using real eigenvalue/eigenvector data obtained from a rotordynamics model. An expression is presented which uses the modal data and the transmitted torque to provide a numerical value of the relative stability of the system. This approach provides a powerful design tool to quickly ascertain the effects of squeeze-film damper bearings, bearing location, and support changes on system stability.

INTRODUCTION

The purpose of this paper is to present a method that is easily and economically applied to turbomachines to predict the effects of shaft flexibility, squeeze-film bearing supports, and static structure configuration on the rotor-bearing/static structure system stability relating to rotor aerodynamic cross coupled stiffness (Alford) forces. The method is general in that systems with general rotor support arrangements and multiple spools can be handled. A major advantage of the method is that it allows machine designers to quickly determine the effects on stability of bearing changes, shaft modifications, and bearing support designs to determine appropriate system designs. This paper presents an expression and analysis methodology for predicting system stability that includes the effects of destabilizing forces, rotor/stator dynamic displacements, internal and external damping, and gyroscopic moments. The expression and methodology presented provides an analysis approach that is simplified but at the same time includes all of the modeling detail needed to perform a valid assessment of system stability.

The method provides a timely and cost effective means to initially screen designs without incurring the high computer costs and large amounts of data reduction time required using complex eigenvalue rotor dynamic analysis programs in a repetitive mode. Specifically, the method uses the results of an undamped lateral critical speed analysis and generalized forces derived from the physical destabilizing forces to develop modal equations of motion for a self-excited system. The solution of these equations is then used to develop a modal dimensionless stability criterion. This criterion requires that the energy absorbed by the system exceed the energy imparted to the rotor by unbalanced torque forces if instability is to be prevented.

The method is intended to supplement the more general analysis techniques which are used for final confirmation of the stability predictions.

F_X, F_{XR}, F_Y, F_{YR}	Aerodynamic forces acting on the rotor N (LBf)
F_{XS}, F_{YS}	Aerodynamic forces acting on the stator N (LBf)
X, Y, X_R, Y_R	Rotor displacements cm (IN.)
X_S, Y_S	Stator displacements cm (IN.)
K_{XY}, K_{YX}	Cross-coupling spring rates N/cm (LBf/IN.)
T	Compressor or turbine stage torque N-cm (LBf-LB)
β	"Alford" coefficient (dim.)
D_P	Stage pitch diameter cm (IN.)
H	Blade height cm (IN.)
P_X, P_Y	Generalized coordinate pair cm (IN.)
ϕ_{XR}, ϕ_{YR}, ϕ_{XS}, ϕ_{YS}	Modal displacements (dim.)
G_X, G_Y	Generalized forces N (LBf)
m	Generalized mass Kg (LBf-SEC^2/IN.)
C	Generalized damping coefficient N-SEC/cm (LBf-SEC/IN.)
k	Generalized stiffness coefficient N/cm (LBf/IN.)
$\{\phi\}$	Mode shape vector (dim.)
$[K]$	Physical stiffness matrix N/cm (LBf/IN.)
ω	Undamped natural frequency (RAD/SEC)
Q	Modal Q-factor (dim.)
N	Number of rotor stages (dim.)
RPM	Design point speed (REV/MIN)
nb	Number of field damping components (casing, frames, rotors)

na	Number of lumped damping components (mounts, bearings, dampers)
Qa	Component Q-factor for lumped damping components (dim.)
Qb	Component Q-factor for field damping components (dim.)
$\dot{\phi}_b$	Spin speeds for field damping components ($\dot{\phi}_b$ is zero for static components) (RAD/SEC)
N_1	Low pressure rotor speed (REV/MIN)
N_2	High pressure rotor speed (REV/MIN)
MSC	Modal Stability Criterion (dim.)

BACKGROUND

A major destabilizing mechanism acting on turbomachinery stages is the Alford aerodynamic cross-coupling stiffness force (ref. 1). In a fixed frame global coordinate system, this force can be modeled by the following equation.

$$\begin{Bmatrix} F_X \\ F_Y \end{Bmatrix} = \begin{bmatrix} 0 & -K_{XY} \\ K_{YX} & 0 \end{bmatrix} \cdot \begin{Bmatrix} X \\ Y \end{Bmatrix} \tag{1}$$

where $K_{XY} = K_{YX} = (T \beta /D_p H)$ N/cm, T is the stage torque, D_p is the pitch diameter of the stage, H is the blade height, and β is the change in thermodynamic efficiency per unit change in blade tip clearance, expressed as a fraction of blade height. The physical rationale for these forces is based on an increase of blade efficiency with decreasing tip clearance. Referring to Figure 1, the displacement of the disc centerline resulting from whirl decreases the blade tip clearance in the direction of the displacement. The efficiency of those blades with reduced clearance is improved resulting in a greater than average torque delivered by those blades with reduced clearances. Conversely, on the side of the disc with increased clearances, a less than average torque is imparted to the rotor by those blades. The integrated effect of the circumferential variation of blade torque results in a net torque in the direction of whirl associated with the vector force described in equation 1. As discussed in references 1 and 2, the cross coupled stiffness can be responsible for self-excited rotor instability at high power levels that is characterized by subsynchronous rotor whirl in the direction of rotation. This subsynchronous whirl is generally associated with the first rotor dominated mode and the stability analysis method to be presented in this paper addresses a mode by mode evaluation approach to ascertain the potential for system instability.

Equation 1 expresses the physical forces acting on the rotor. It can be extended to include the forces acting on the case (stator) as follows.

$$
\begin{Bmatrix} F_{XR} \\ F_{YR} \\ F_{YR} \\ F_{XS} \\ F_{YS} \end{Bmatrix} = \begin{bmatrix} 0 & -K_{XY} & 0 & K_{XY} \\ K_{YX} & 0 & -K_{YX} & 0 \\ 0 & K_{XY} & 0 & -K_{XY} \\ -K_{YX} & 0 & K_{YX} & 0 \end{bmatrix} \cdot \begin{Bmatrix} X_R \\ Y_R \\ X_S \\ Y_S \end{Bmatrix}
\tag{2}
$$

These forces will be used in conjunction with the gyroscopically stiffened modes obtained from a real eigenvalue/eigenvector analysis to develop a stability criterion. For a given mode obtained from the real mode set, define P_X and P_Y as the modal coordinate pair describing the generalized response in the vertical and horizontal planes of the system. More will be said later in this paper about the incorporation of gyroscopic effects in the modal data.

The rotor and stator modal displacements at a given stage can then be used to define the physical destabilizing forces acting on the rotor and stator as follows:

$$
\begin{aligned}
F_{XR} &= -K_{XY} (Y_R - Y_S) = -K_{XY}P_Y (\phi_{YR} - \phi_{YS}) \\
F_{YR} &= K_{YX} (X_R - X_S) = K_{YX}P_X (\phi_{XR} - \phi_{XS}) \\
F_{XS} &= K_{XY} (Y_R - Y_S) = -F_{XR} \\
F_{YS} &= -K_{YX} (X_R - X_S) = -F_{YR}
\end{aligned}
\tag{3}
$$

The total generalized forces acting in the X and Y directions can be written

$$
\begin{aligned}
G_X &= -K_{XY}P_Y (\phi_{YR}-\phi_{YS}) \phi_{XR} + K_{XY}P_Y (\phi_{YR} - \phi_{YS}) \phi_{XS} = \\
&= -K_{XY}P_Y (\phi_{YR} - \phi_{YS}) (\phi_{XR} - \phi_{XS})
\end{aligned}
\tag{4}
$$

$$
\begin{aligned}
G_Y &= K_{YX}P_X (\phi_{XR} - \phi_{XS}) \phi_{YR} - K_{YX}P_X (\phi_{XR} - \phi_{XS}) \phi_{YS} = \\
&= K_{YX}P_X (\phi_{XR} - \phi_{XS}) (\phi_{YR} - \phi_{YS})
\end{aligned}
$$

If circular whirl is assumed,

$$
\begin{aligned}
\phi_R &= \phi_{XR} = \phi_{YR} \\
\phi_S &= \phi_{XS} = \phi_{YS}
\end{aligned}
\tag{5}
$$

Then the generalized forces are

$$
\begin{aligned}
G_X &= -K_{XY}P_Y (\phi_R - \phi_S)^2 \\
G_Y &= K_{XY}P_X (\phi_R - \phi_S)^2
\end{aligned}
\tag{6}
$$

The equations of motion for the modal coordinate pair are

$$
\begin{aligned}
m\ddot{P}_X + C\dot{P}_X + k\,P_X &= G_X \\
m\ddot{P}_Y + C\dot{P}_Y + k\,P_Y &= G_Y
\end{aligned}
\tag{7}
$$

Combining these equations and eliminating P_Y,

$$\frac{d^4 P_X}{dt^4} + \frac{2C}{m} \frac{d^3 P_X}{dt^3} + \left(\frac{2k}{m} + \frac{c^2}{m^2}\right)\frac{d^2 P_X}{dt^2} + \frac{2Ck}{m^2} \frac{dP_X}{dt} \tag{8}$$

$$+ \left(\frac{k^2}{m^2} + \frac{K^2_{XY}(\phi_R - \phi_S)^4}{m^2}\right) P_X = 0$$

For a solution, assume $P_X = p_x e^{st}$ and upon substitution, the following characteristic equation is obtained.

$$s^4 + A_3 s^3 + A_2 s^2 + A_1 s + A_0 = 0 \tag{9}$$

The complex eigenvalues of this equation define the stability boundaries of the system. Specifically, a root with a positive real part indicates an unstable system. Per the Routh stability analysis, an inspection of the coefficients of the characteristic equation determines whether the motion is stable or unstable

For a stable system,

$$A_1 A_2 A_3 > A_1^2 + A_3^2 A_0 \tag{10}$$

Evaluating the terms,

$$A_1 A_2 A_3 = \frac{2Ck}{m^2}\left(\frac{2k}{m} + \frac{c^2}{m^2}\right)\frac{2C}{m}$$

$$= \frac{4C^2 k}{m^3}\left(\frac{2k}{m} + \frac{c^2}{m^2}\right)$$

$$A_1^2 + A_3^2 A_0 = \frac{4C^2 k^2}{m^4} + \frac{4C^2}{m^2}\left(\frac{k^2}{m^2} + \frac{K^2_{XY}(\phi_R - \phi_S)^4}{m^2}\right)$$

Then

$$\frac{c^2}{m} > \frac{K^2_{XY}(\phi_R - \phi_S)^4}{k}$$

Equation 10 can be written as

$$C > \frac{K_{XY}}{\omega}(\phi_R - \phi_S)^2$$

or $\quad k > K_{XY}(\phi_R - \phi_S)^2 Q \tag{11}$

where $\omega = \sqrt{k/m}$ = undamped natural frequency,

and $Q = k/C\omega =$ modal Q-factor.

Expressing the relative modal displacement on a per stage basis

and the cross-coupling stiffness in terms of the rotor speed and the HP per stage at the design point leads to the following equation.

For stability,

$$\frac{2PE}{\dfrac{713,361}{RPM} \, Q \displaystyle\sum_{i=1}^{N} \dfrac{\beta_i HP_i}{D_{P_i} H_i} (\phi_{R_i} - \phi_{S_i})^2} > 1.0 \quad (12)$$

where $PE = 1/2 \, \{\phi\}^T [K]\{\phi\} = 1/2 \, k =$ modal potential energy and $N =$ the number of rotor stages. Equation 12 represents an energy balance expressed in terms of the pertinent modal parameters for a system mode of vibration and the physical destabilizing forces. If English units are used, then the constant 713,361 RPM-cm-N/HP becomes 63,025 RPM-IN-LB/HP. The accurate calculation of the modal or generalized Q-factor is key to the use of equation 12 for evaluating system stability. It must reflect the effects of both external and internal damping and the modal participation of the various engine components.

The modal Q-factor is given by equation A10 in the Appendix. Substituting this equation into equation 12 yields the following modal stability criterion (MSC). For stability,

$$\frac{2 \displaystyle\sum_{a=1}^{na} \dfrac{PE_a}{Q_a} + \displaystyle\sum_{b=1}^{nb} \left(1 - \dfrac{\dot{\phi}_b}{\omega}\right) \dfrac{PE_b}{Q_b}}{\dfrac{713,361}{RPM} \displaystyle\sum_{i=1}^{N} \dfrac{\beta_i HP_i}{D_{P_i} H_i} (\phi_{R_i} - \phi_{S_i})^2} > 1.0 \quad (13)$$

Note that squeeze-film damper elements contribute lumped damping and are included in the summation a=1, 2, 3, ..., na. As an approximation, they are modeled as soft springs in the system vibration analysis and a conservative component Q-factor of 3.0 can be used, although a more exact value can be calculated.

GYROSCOPIC EFFECTS AND ROTOR INTERNAL DAMPING

Figure 2 shows an example of a typical engine system vibration model used to generate modal data for the MSC. This model represents a single plane of a demonstrator engine and is an assemblage of substructure (span) and spring-type elements. It can be built very rapidly and is easily altered and interactively run to generate modal data for MSC evaluation of a wide range of alternative system designs. The span element type, represented by solid lines in Figure 2, includes both flexibility and mass properties and models casings, rotors, and

frames. The spring-type elements model bearings, mounts, and dampers. Gyroscopic moments are incorporated through spin and whirl frequency dependent terms in the mass matrices of the substructures. Note that while the modal data is obtained from an analysis which models a single plane of the engine, it does reflect whirling motion of the rotors. Consider the consequence of cross-axis gyroscopic coupling: (1) lateral motions of the rotor are not planar-the rotor center motion describes a circular orbit, if rotational symmetry prevails; (2) each free vibration mode of the equivalent non-rotating shaft of the planar model is split into two modes which are distinguishable by the sense of whirl motion (relative to the shaft spin). These are forward and backward whirling modes, and since the Alford instability mechanism drives forward whirling modes, the planar model is constrained to provide forward whirling modes for the reference rotor. Figure 3 shows the Campbell diagram (map of natural frequencies vs spin speeds), for the model of Figure 2, referenced to high pressure rotor spin speeds. The frequency lines represent system modes involving forward whirl of the high pressure rotor and backward whirl of the low pressure rotor. The latter are a consequence of counterrotating rotors, and decreasing natural frequency (due to gyro softening) with increasing high pressure rotor speed reflects dominant low pressure rotor participation. Figure 4 shows examples of mode shapes for two high pressure rotor subsynchronous modes at the 13,226 RPM N_2/-11,340 RPM N_1 design point for the Campbell diagram of Figure 3. The 3131^2 cycle/min (CPM) mode is a fan shaft bending mode and the 8303 CPM mode is a core rotor bending mode, with the core rotor out-of-phase with the core case. For these two modes, the spin speed to whirl frequency ratios $\dot{\phi}_b/\omega$ for the high and low pressure rotors are equal to (4.22, -3.62) and (1.59, -1.36), respectively. The MSC evaluations are based on a mode by mode evaluation at the design point (design speeds and reference rotor torque). The MSC values are calculated for each forward whirl high pressure rotor mode and the minimum value is the basis for the rotor system stability prediction. Since the destabilizing effects of the aerodynamic cross-coupling forces are generally much more significant for the high pressure rotor than for the low pressure rotor, the former is considered as the reference rotor. Hence, the index i in equation 13 ranges over the stages for the high pressure rotor; both power absorption (compressor stages), and power generation (turbine stages) are included in the summation. It will be noted that single mode evaluation is acceptable because the cross-axis stiffness associated with the Alford forces is relatively small and, therefore, little loss in accuracy results from the use of the original mode shapes in the stability calculations.

The incorporation of the modal Q-factor in the MSC results in the implicit inclusion of rotor hysteresis or rotary damping which can be destabilizing if the rotor is undergoing subsynchronous vibration. The spin speed to whirl frequency ratios obtained from the system vibration analysis provide the data needed to correctly incorporate the effects of rotor internal damping in the generalized or modal damping for the mode. Hence, the modal Q-factor provides the effective system damping needed to correctly define the energy absorbed by the turbomachine at resonance.

EXAMPLE STABILITY CALCULATION AND ROTOR WHIRL EXPERIENCE

To demonstrate the calculation method, the MSC values are calculated for each

natural frequency involving high pressure rotor forward whirl at the design point

for the engine model of Figure 2. These natural frequencies are calculated up to the HP rotor synchronous frequency and correspond to the intersection of the Campbell diagram frequency lines and a vertical line passing through the reference rotor design speed (Figure 3). They occur at 1118, 1554, 1665, 3131, 4034, 5966, 6654, 8303, 10632, and 12580 CPM.

For example, for the 8303 CPM high pressure rotor bending mode, the numerator of equation 13 is equal to 122,708. In general, $1 < \beta < 2$. Setting β equal to 2.0 for each stage, the term

$$\sum_{i=1}^{N} \frac{\beta_i HP_i}{DP_i H_i} (\phi_{Ri} - \phi_{Si})^2$$

of equation 13 is equal to 1569 HP/cm^2.

As previously mentioned, the summation i=1, 2, ..., N encompasses both the compressor and turbine stages of the high pressure rotor. Then at the $N_2 =$ 13,226 RPM design speed of the high pressure rotor:

The MSC is equal to $\dfrac{123{,}067 \ N/cm}{\dfrac{713{,}361}{13226}(1569) \ N/cm} = 1.45$

Table 1 provides the MSC and modal Q-factor for the design point modes. This table shows that the minimum value for the MSC occurs for the 8303 CPM mode and that the system is predicted to be stable.

The modal stability criteria has shown good correlation with experience for various General Electric Aircraft engines.

CONCLUSIONS

The MSC provides a convenient and quick means to perform a rotor stability analysis using modal data readily available from planar system vibration models. It includes all of the significant parameters (gyroscopic moments, damping, rotor/stator relative displacements), and modeling detail needed to perform a valid assessment of rotor stability related to Alford forces. The assumption of circular whirl means that the stabilizing effects of non-axisymmetric rotor and/or engine support stiffness are not included, and this may result in built-in conservatism, depending on the characteristics of the engine system modes.

REFERENCES

1. J. S. Alford, "Protecting Turbomachinery from Self-Excited Rotor Whirl," ASME Trans. Journal of Engineering for Power, Series A, pp. 333-344, Oct. 1965.

2. Childs, D. W.,"The Space Shuttle Main Engine High-Pressure Fuel Turbopump Rotordynamic Instability Problem", ASME Trans. Engineering for Power, Vol. 100, No. 1, January 1978.

3. Gunter, E. J., "Dynamic Stability of Rotor-Bearing Systems," NASA SP-113, U.S. Government Printing Office, Washington,   D. C., 1966.

4. Ehrich, F. F., "Shaft Whirl Induced by Rotor Internal Damping," Journal of Applied Mechanics, June 1964, pp. 279-282.

TABLE I - MODAL STABILITY AND Q-FACTOR VALUES CALCULATED AT THE DESIGN POINT* FOR THE ENGINE MODEL OF FIGURE 2

NATURAL FREQUENCY (CPM)	MODAL-Q	MSC
1118	12.5	1657
1544	12.4	2643
1665	15.1	1112
3131	20.7	12
4034	16.1	58.9
5966	21.4	246
6654	15.3	7.5
8303	19.3	1.45
10632	16.5	53.7
12580	18.5	6.0

* N_1 = 11340 RPM/N_2 = 13226 RPM
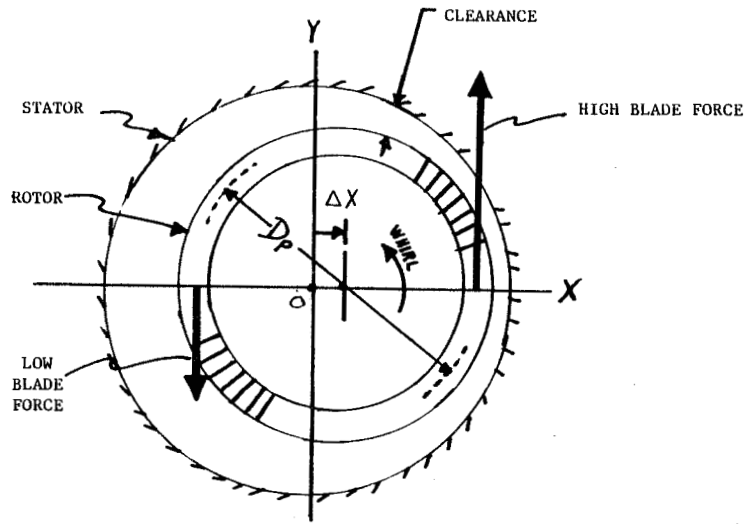
ROTOR DISK ECCENTRIC TO STATOR IN X DIRECTION
PRODUCES NET FORCE IN Y DIRECTION

FIGURE 1 - ALFORD INSTABILITY MECHANISM
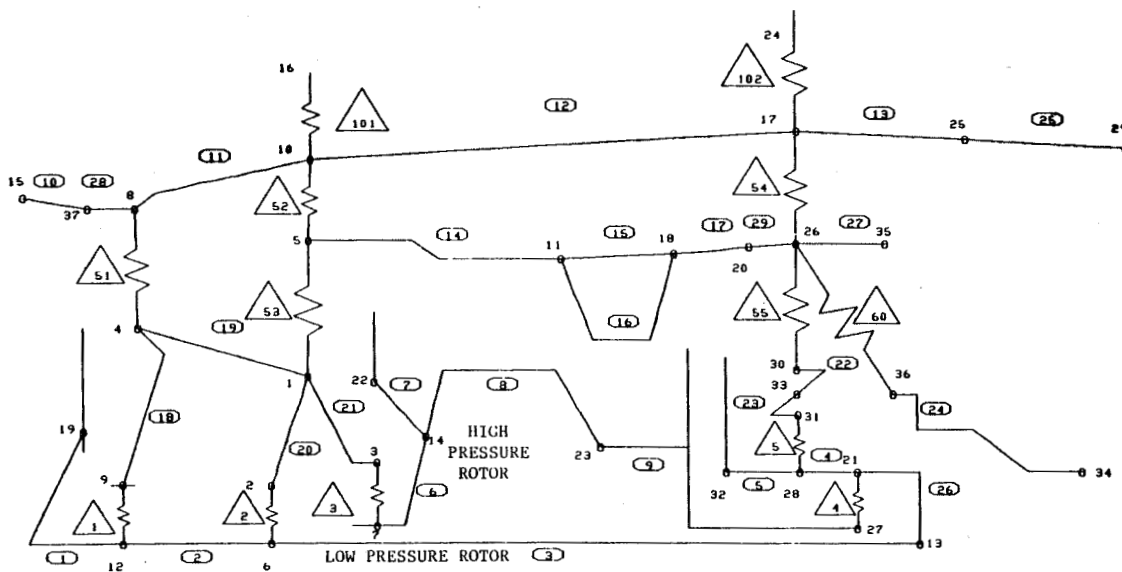

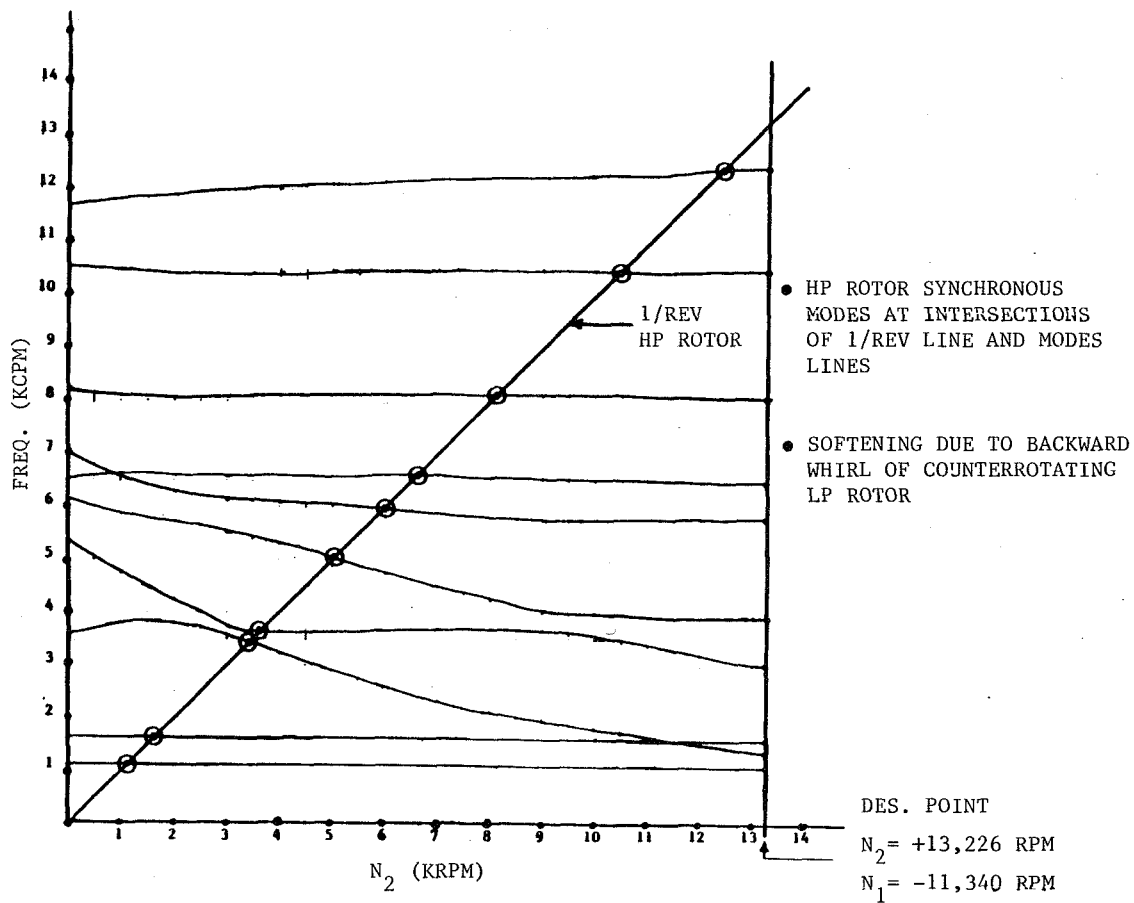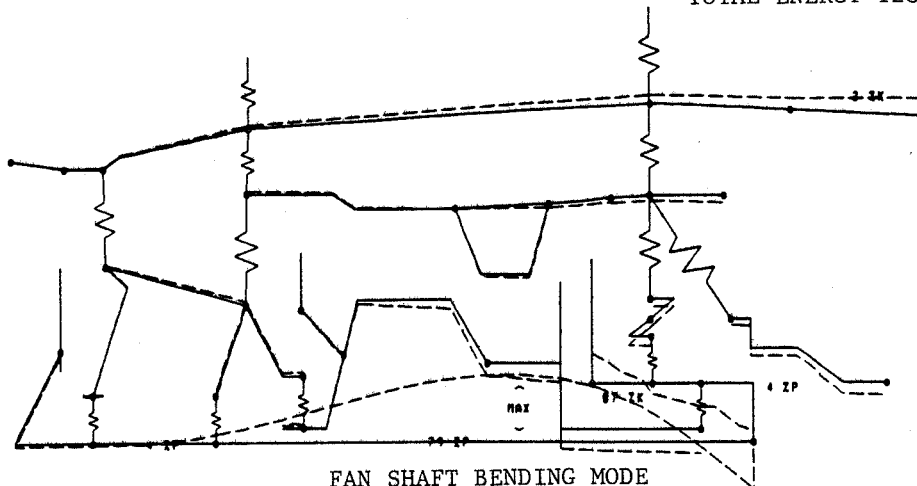FIGURE 2 - SYSTEM VIBRATION MODEL OF A DEMONSTRATOR ENGINE

294

FIGURE 3 – CAMPBELL DIAGRAM
         FORWARD WHIRL MODES FOR HP ROTOR
         BACKWARD WHIRL MODES FOR LP ROTOR

HP ROTOR FORWARD WHIRLING MODE AT
THE DESIGN POINT

N1=-11340, N2=13226   RPM=3131.3
                             TOTAL ENERGY 128744
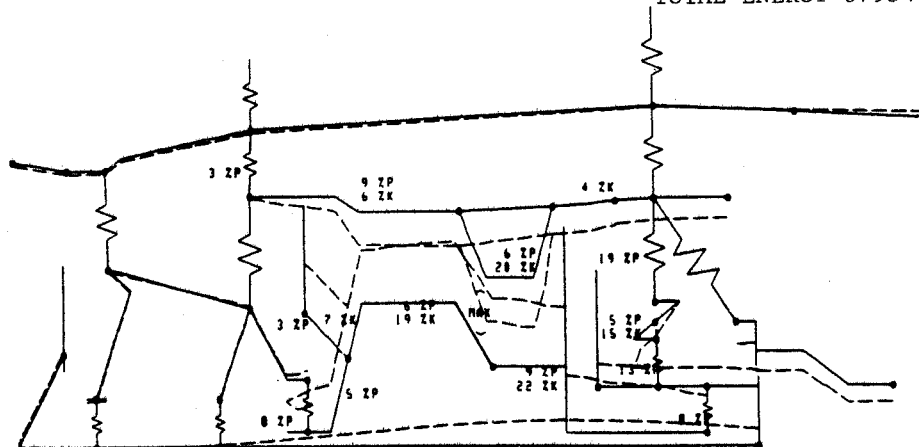

FAN SHAFT BENDING MODE

$$R_{LP} = \frac{-11340}{3131} = -3.62$$

$$R_{HP} = \frac{13226}{3131} = +4.22$$

HP ROTOR FORWARD WHIRLING MODE
AT THE DESIGN POINT

N1=-11340, N2=13226   RPM=8302.6
                             TOTAL ENERGY 679347

CORE BENDING MODE

$$R_{LP} = \frac{-11340}{8303} = -1.36$$

$$R_{HP} = \frac{13226}{8303} = +1.59$$

FIGURE 4 - EXAMPLES OF HIGH PRESSURE ROTOR SUBSYNCHRONOUS MODES

APPENDIX

DEVELOPMENT OF MODAL Q-FACTOR EQUATION

The equation for the modal Q-factor is developed by summing the damping contributions of the engine components (field damping for casings, frames, and rotor component structures, and lumped damping for mounts, bearings, and squeeze-film dampers).

The Q-factor for the i-th component is defined as

$$Q_i = \frac{2\pi PE_i'}{E_{Di}} \tag{A1}$$

where PE_i' is the physical strain energy in the component and E_{Di} is the energy dissipated.

Consider the work done on the system at resonance by an excitation force P at point j expressed in terms of modal data for the system.

$$W_{IN} = \pi P_j \phi_j (SF) \tag{A2}$$

where ϕ_j is the modal displacement at point j and SF is a scale factor relating the modal displacement to the physical displacement.

From equation A1, the energy dissipated by the engine components

is

$$W_D = 2\pi(SF)^2 \sum_{i=1}^{n} \frac{PE_i}{Q_i} \tag{A3}$$

where n is the number of components and PE_i is the modal strain energy in the i-th component.

Equating the work done on the system to the energy dissipated leads to a solution for the modal scale factor SF.

$$SF = \frac{\pi P_j \phi_j}{2\pi \sum_{i=2}^{n} \frac{PE_i}{Q_i}} = \frac{P_j \phi_j}{2 \sum_{i=1}^{n} \frac{PE_i}{Q_i}} \tag{A4}$$

where ϕ_j is the modal displacement at point j.

In reality, the modal scale factor is the modal participation at resonance, or

$$SF = \frac{\tilde{f}}{k} Q \tag{A5}$$

where $\tilde{f} = P_j \phi_j$ = the generalized force and k is the generalized stiffness.

Hence,

$$Q = (SF)\frac{k}{\tilde{f}} = \frac{P_j \phi_j}{2\sum\limits_{i=1}^{n} \dfrac{PE_i}{Q_i}} \frac{2PE}{\tilde{f}} = \frac{PE}{\sum\limits_{i=1}^{n} \dfrac{PE_i}{Q_i}} \qquad (A6)$$

Equation A6 provides the modal Q-factor for the system reflecting the damping contributions of the static structures and the rotor component structures. However, in the latter case, the rotors are treated as stationary component structures since the effects of spin and whirl have not been included. Hence, the internal or hysteretic damping associated with a spinning and whirling rotor has been neglected. This damping mechanism is characterized by an internal friction force caused by the rate of change of strain within the rotor. This internal friction force can be represented with the viscous damping model derived in references 3 and 4 as

$$F_t = -C_t \delta(\omega - \dot{\phi}) \qquad (A7)$$

where C_t is the viscous damping coefficient for a stationary rotor, $\dot{\phi}$ is the spin speed, ω is the whirl frequency, and δ is the whirl displacement.

Equation A7 represents the follower force (tangential force which leads the whirl displacement δ by 90°) F_t in a rotating coordinate system fixed to the rotor. An equivalent damping coefficient is derived as follows.

$$F_t = -C_{EQ}\omega\delta = -C_t\delta(\omega-\dot{\phi}) = -C_t\omega\delta(1-\dot{\phi}/\omega) \qquad (A8)$$

Hence, $C_{EQ} = C_t(1-\dot{\phi}/\omega)$

If Q_R is the component Q-factor for a stationary rotor corresponding to C_t, then an equivalent field Q-factor Q_{EQ} for a whirling and spinning rotor of stiffness k_R can be defined as follows.

$$C_{EQ} = \frac{1}{Q_{EQ}}\frac{k_R}{\omega} = \frac{1}{Q_R}\frac{k_R}{\omega}(1-\dot{\phi}/\omega)$$

$$\text{or} \qquad Q_{EQ} = \frac{Q_R}{(1-\dot{\phi}/\omega)} \qquad (A9)$$

Notice that the equivalent Q-factor Q_{EQ} for the rotor is negative when the rotor speed $\dot{\phi}$ is greater than the whirling speed ω. Physically this means that the damping force F_t acts in the direction of whirling for subsynchronous vibration and is thus destabilizing.

Incorporating the expression for the rotor Q-factor into equation A6 yields the following equation for the modal Q-factor which includes the effects of spinning and whirling rotors.

$$Q = \cfrac{PE}{\sum_{a=1}^{na} \cfrac{PE_a}{Q_a} + \sum_{b=1}^{nb} (1-\dot{\phi}_b/\omega) \cfrac{PE_b}{Q_b}} \qquad (A10)$$

PE   =   total system modal potential energy

na   =   number of lumped damping components (mounts, bearings, dampers)

PE_a =   modal strain energy for lumped damping components

Q_a =   component Q-factors for lumped damping components

nb   =   number of field damping components (casings, frames, rotors)

$\dot{\phi}_b$ =   spin speeds for field damping components ($\dot{\phi}_b$ is zero for static components)

PE_b =   modal strain energy for field damping components

Q_b =   component Q-factors for field damping components